J Radioanal Nucl Chem (2016) 310:1353–1360
DOI 10.1007/s10967-016-4934-y

Enhanced accumulation of U(VI) by *Aspergillus oryzae* mutant generated by dielectric barrier discharge air plasma

Wencheng Song[1,2] · Xiangxue Wang[2,3] · Wen Tao[2] · Hongqing Wang[4] · Tasawar Hayat[5,6] · Xiangke Wang[2,3,5]

Received: 31 May 2016 / Published online: 15 July 2016

Abstract *Aspergillus oryzae* was isolated from radionuclides' contaminated soils, and dielectric barrier discharge plasma was used to mutate *A. oryzae* to improve bioremediation capability of U(VI) pollution. The maximum accumulation capacities of U(VI) on mutated *A. oryzae* was 627.4 mg/g at $T = 298$ K and $pH = 5.5$, which was approximately twice than that of raw *A. oryzae*. XPS analysis indicated that U(VI) accumulation on mutated *A. oryzae* was largely attributable to nitrogen- and oxygen-containing functional groups on fungal mycelia. The mutated *A. oryzae* can be harnessed as bioremediation agents for radionuclides pollution.

✉ Wencheng Song
wencsong@cmpt.ac.cn

✉ Xiangke Wang
xkwang@ncepu.edu.cn

1 Center of Medical Physics and Technology, Hefei Institutes of Physical Science, Chinese Academy of Sciences, Hefei 230031, People's Republic of China

2 School of Environment and Chemical Engineering, North China Electric Power University, Beijing 102206, People's Republic of China

3 Collaborative Innovation Center of Radiation Medicine of Jiangsu Higher Education Institutions, and School for Radiological and Interdisciplinary Sciences, Soochow University, Suzhou 215123, People's Republic of China

4 School of Chemistry and Chemical Engineering, University of South China, Hengyang 421001, Hunan, People's Republic of China

5 NAAM Research Group, Faculty of Science, King Abdulaziz University, Jeddah 21589, Saudi Arabia

6 Department of Mathematics, Quaid-I-Azam University, Islamabad 44000, Pakistan

Keywords Accumulation · *Aspergillus oryzae* · Mycelia · U(VI)

Introduction

Pollution caused by radionuclides has attracted much attention as a result of the development of nuclear science and technology. The presence of radionuclides in the environment would hazard human health [1–4]. Conventional technologies have been developed for the removal of radionuclides from the environment. For example, coagulation-flocculation [5], precipitation [6, 7], adsorption [8–10], ion exchange [11], and membrane filtration [12] have been gradually employed for the treatment of radionuclides contaminated wastewaters. Although these methods have been widely used, they have many limitations, such as complex measurement and operation procedures, high cost, and easily caused secondary pollution [13]. For the past few years, bioremediation using microorganisms is more advantageous for the removal of radionuclides from the radioactive environment owing to its little by-product, high-performance, and low-cost technology [14, 15]. Therefore, plenty of microorganisms have been used for removal of radionuclides from solution, such as bacteria [16, 17], yeasts [18], fungi [19, 20], and algae [21]. Among them, fungi are suitable bioremediation agents with favorable prospects for the enrichment of radionuclides from liquid wastes [19]. In order to increase the bioremediation capacity of microorganisms, many mutation methods have been used. For example, heavy-ion irradiation mutagenesis of *Nannochloropsis* greatly improved lipid productivity and TAG content [22]; Hydroxylamine hydrochloride and UV light were used to mutate *Penicillium funiculosum* and adsorption

performance of U(VI) on *P. funiculosum* was greatly improved [23].

Atmospheric pressure dielectric barrier discharge (DBD) air plasma, one of the electrical discharge plasma technologies, generates a mixture of reactive species, such as charged particles, free radicals, excited neutral species, high electric field, and UV radiation [24]. It was demonstrated that atmospheric and room temperature plasma can dramatically alter the DNA of microorganisms, which suggests that it is a forceful tool to mutate microorganisms with the advantages of easy operation, safety, low cost and wide application [25]. Atmospheric and room temperature plasma was successfully employed to mutate *Klebsiella pneumoniae*, *Candida shehatae, Streptomyces avermitilis*, *Rhodosporidium toruloides* [26–29].

In this study, radionuclides-resistant *Aspergillus oryzae* (*A. oryzae*) was isolated from radionuclides' contaminated soils in China and DBD plasma was used to mutate *A. oryzae* in order to improve U(VI) accumulation. Also, accumulation of U(VI) on mutated *A. oryzae* as affected by experimental parameters like pH, ionic strength, mycelia content, and temperature were studied.

Experimental

Strain isolation and identification

The tested fungal mycelia isolated from radionuclides' contaminated sites (Huajia County, Gansu Province, PR China), near to a nuclear weapon test. 2.0 g soil sample were suspended in 100 ml of sterilized water, and 2 ml of the suspension was added to sterilized water to obtain desired dilutions up to 10^{-7}. 100 µl different dilutions were spread on potato dextrose agar (PDA) plates which contained 400 mg/g U(VI). The inoculated plates were incubated at room temperature for 2–4 days. Then, the largest colony on PDA plates was selected and purified, and identified by molecular methods. DNA was extracted from growing mycelium [30]. The universal fungal primers ITS1/ITS4 was used to amplify ITS region gene. The parameters of polymerase chain reaction (PCR) were 94 °C for 6 min, followed by 30 cycles of 94 °C for 40 s, 56 °C for 30 s, 72 °C for 1 min, and elongation at 72 °C for 10 min. The amplification products were followed by DNA sequencing (Sangon, Shanghai), and then the sequence was submitted to the BlastN (http://blast.ncbi.nlm.nih.gov/) for the homology analysis.

Strain mutagenesis experiments

DBD plasma was generated at 60 V and power of 80–140 W between the two quartz dielectric barriers with the gap of 3 mm. Spore suspension of the strain was harvested from 6 days old PDA slants and was appropriately diluted for 10^7/ml. After DBD plasma treatment at room temperature for 6 min, the 100 µl spore suspension was taken to PDA plates contained 600 mg/g U(VI). Then, the Erlenmeyer flasks (250 ml) containing 100 ml of PDA medium was inoculated by the largest mutated colony. Subsequently, the sample was cultured under 28 °C for 3 days. Mid-log phase mycelia were collected, washed with sterilized water, freeze-dried, and ground into particles less than 0.45 mm for accumulation experiments.

Characterization of fungal mycelia

The surface morphology of fungal mycelia was investigated by SEM (JEOL JSM-6330F, Japan). The mycelia and the U(VI) loaded mycelia were solidified with 2.0 % glutaraldehyde and then 1.0 % osmic acid, washed with distilled water, and then dehydrated through a graded ethanol series, finally critical-point-dried, gold-coated with stubs for SEM analysis. In addition, the functional groups of fungal mycelia were characterized by FTIR (Perkin Elmer 100, USA), potentiometric acid–base titration (DL50 Automatic Titrator, Switzerland), and XPS (Thermo ESCALAB 250, USA).

Accumulation procedures

All the accumulation experiments were carried out using the batch technique. The suspensions of different concentrations of mycelia, U(VI), and NaCl solution were added to 250 ml Erlenmeyer flasks. Afterwards, the suspensions were shocked for 48 h to achieve accumulation equilibrium, and mycelia were separated by centrifugation. The counts of U(VI) was determined by Liquid Scintillation counting using a Packard 3100 TR/AB Liquid Scintillation Analyzer (Perkin-Elmer). The accumulation percent (Accumulation % $= (C_0 - C_e) \times 100\ \%/C_e$) and amounts of U(VI) accumulation ($Q = (C_0 - C_e) \times V/m$) were derived from initial concentration (C_0), equilibrium concentration (C_e), volume of suspension (V), and mass of mycelia (m). The effect of pH on the accumulation percentage was investigated in the pH range of 2.0–10.0. The medium pH was adjusted with dilute HCl or NaOH using a pH meter (PB-10, Sartorius, Germany) at 25 °C. To optimize the mycelia content, batch experiments were conducted using different amounts of mycelia from 0.01 to 0.8 g/l at pH 5.5. To investigate the influence of ionic strength on U(VI) accumulation, NaCl was employed as background electrolyte and varied from 0.01 to 0.06 mol/l. To determine the effect of initial U(VI) concentration on the accumulation capacity, the initial concentration of U(VI) was varied

from 10 to 300 mg/l at pH 5.5. All tests were conducted in triplicate.

Results and discussion

Identification and characterization of the fungus

595 bp sequence of ITS gene was analyzed using the online database (NCBI website) for the homology analysis in order to identify the species of the isolated fungus. The blast analysis and alignment with different fungal sequences in NCBI database showed the sequence exhibited 99 % identity with that of *A. oryzae* (GenBank accession no. JN561266.1 and HM145964.1). Based on these results, the isolate was identified as *A. oryzae*.

The SEM micrographs of mutated *A. oryzae* and U(VI) loaded mutated *A. oryzae* (mutated *A. oryzae*-U) are shown in Fig. 1. It was observed that the surface morphology of mutated *A. oryzae* considerably changed after U(VI) accumulation. Compared with raw fungal mycelia (Fig. 1a), U(VI) loaded fungal mycelia cells looked obviously more plump (Fig. 1b). The alteration in morphology may, to a certain extent, result from increasement of the fungal cell inclusions and secretion of the extra cellular polymeric substance, in response to U(VI) toxicity [31].

The pH_{pzc} value indicates that the *A. oryzae* and mutated *A. oryzae* displays a great buffering capacity across the pH range in 0.01 mol/l NaCl solution (Fig. 2a). At pH $<$ pH_{pzc}, the fungal surface charge is positive. Whereas, the fungal surface charge is negative at pH $>$ pH_{pzc}. The value of pH_{pzc} of mutated *A. oryzae* is 5.8, and the buffering-like zone between pH 4.0 and pH 8.0 appears where the pH declines gradually. The zone of mutated *A. oryzae* is wider than that of *A. oryzae*, which indicates mutated *A. oryzae* has more functional groups [32].

Effect of mycelia content

Figure 2b showed that mycelia concentration obviously affected the U(VI) accumulation on mutated *A. oryzae*. The accumulation of U(VI) sharply increased as mutated *A. oryzae* concentration increased. That is because functional groups which related to accumulation process increased when mutated *A. oryzae* concentration ascended. Oppositely, Q decreased when mutated *A. oryzae* concentration increased, because the competition among mutated *A. oryzae* would decrease available functional groups on mutated *A. oryzae*, which resulted in Q decreasing [33].

Effect of pH

As shown in Fig. 3a, *A. oryzae* and mutated *A. oryzae* accumulation U(VI) was affected by pH. The accumulation increases significantly when the pH value increases from 2.0 to 5.0 and maintains the high level between pH 5.0 and 7.0, then decreases steeply in the pH range of 7.0–10. At pH 6.0 approximately 80 % U(VI) accumulated on mutated *A. oryzae*, which is approximately twice than that of *A. oryzae*. These could be attributed to the electrostatic interaction between U(VI) and fungal mycelia. The distribution of different U(VI) species in aqueous as a function of solution pH is given in Fig. 3b. U(VI) exists as UO_2^{2+} at pH $<$5.0, $(UO_2)_3(OH)_5^+$ and $(UO_2)_4(OH)_7^+$ at pH 5.0–8.0, and $UO_2(OH)_3^-$ at pH $>$8.0 [34]. The surface of mutated *A. oryzae* was positively charged at pH $<$5.8 (Fig. 2a). Thereby, the electrostatic repulsion between mutated *A. oryzae* and UO_2^{2+} leads to the low accumulation at pH $<$5.0. The high accumulation of U(VI) at pH 5.0–8.0 can be attributed to the strong electrostatic attraction between positively charged U(VI) species and negatively charged mycelia. The repulsion between $UO_2(OH)_3^-$ and the negatively charged mycelia leads to a drop of U(VI) accumulation at pH $>$8.0 [34, 35].

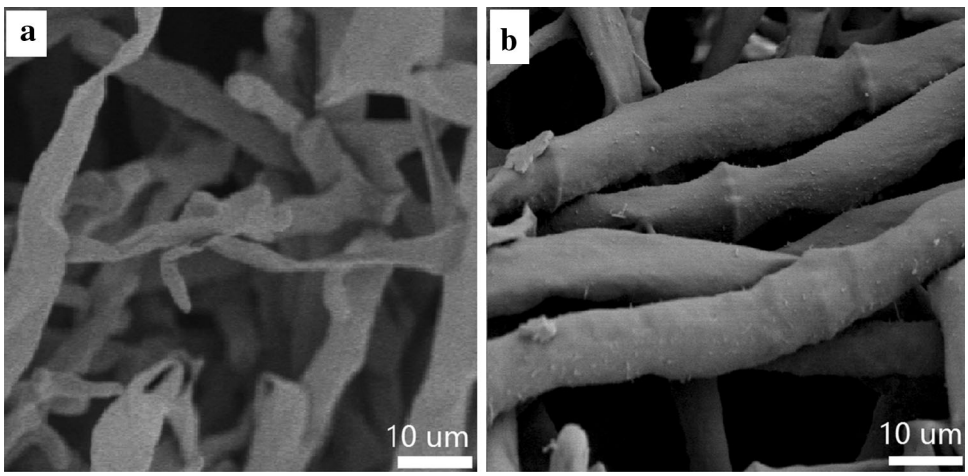

Fig. 1 SEM images of mutated *A. oryzae* (**a**) and mutated *A. oryzae*-U (**b**)

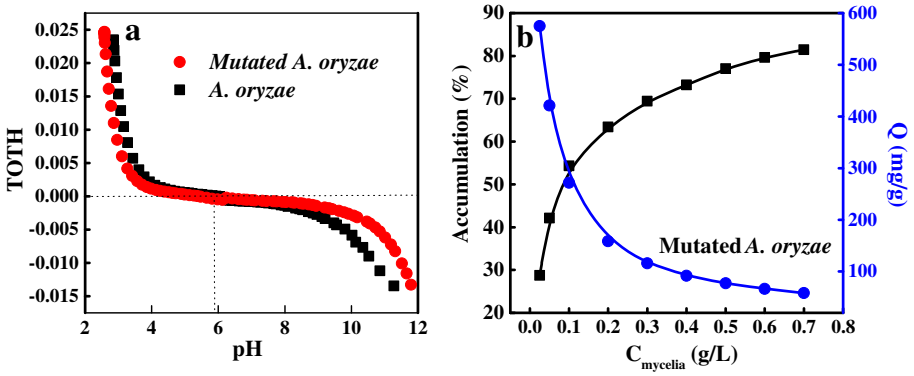

Fig. 2 Potentiometric titration of *A. oryzae* and mutated *A. oryzae* (**a**); the effect of mycelia content on U(VI) accumulation to mutated *A. oryzae* (**b**), T = 298 K, $C_{[U(VI)]initial}$ = 50 mg/l

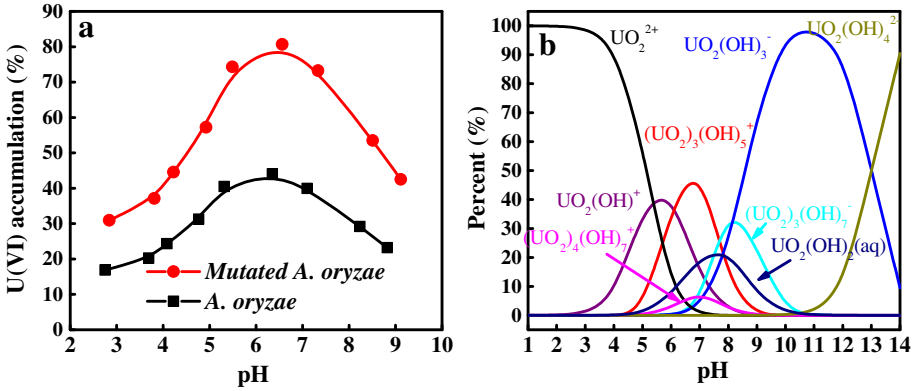

Fig. 3 Effect of pH on U(VI) accumulation to *A. oryzae* and mutated *A. oryzae* (**a**); relative distribution of U(VI) species as a function of pH based on the equilibrium constants (**b**). T = 298 K, m/V = 0.6 g/l, $C_{[U(VI)]initial}$ = 50 mg/l

Effect of ionic strength

It also is found that U(VI) accumulation on mycelia is clearly dependent on NaCl concentrations at pH 5.5 (Fig. 4a). The U(VI) accumulation on *A. oryzae* and mutated *A. oryzae* percentage decreases as NaCl concentration increased. This phenomenon could be interpreted by ion-exchange mechanism: the formed electrical double layer complexes between U(VI) and the fungal mycelia favor U(VI) accumulation as the content of NaCl decreased, indicating ionic interaction was the main interaction between U(VI) and functional groups [36]. Additionally, the increasing ionic strength may result in mycelia aggregation and thereby reduced the available sites to U(VI) on the surface of mycelia.

Accumulation Isotherms

Radioactive wastewater is usually the acid medium. Hence, U(VI) accumulation isotherms of *A. oryzae* and mutated *A. oryzae* was estimated at pH 5.5 and 298 K. As shown in Fig. 4b, the amounts of U(VI) accumulation on *A. oryzae* and mutated *A. oryzae* enhanced quickly as U(VI) concentration increased. To characterize the accumulation

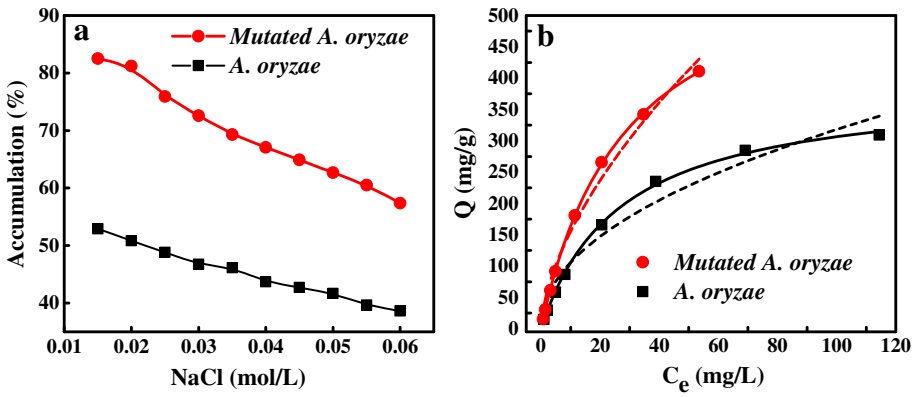

Fig. 4 Effect of ionic strength on U(VI) accumulation by *A. oryzae* and mutated *A. oryzae* (**a**), T = 298 K, m/V = 0.6 g/l, $C_{[U(VI)]initial}$ = 50 mg/l; The isotherms of U(VI) on *A. oryzae* and mutated *A. oryzae*, the *solid line* stands for Langmuir model and the *dash line* stands for Freundlich model (**b**), pH = 5.5, m/V = 0.6 g/l, T = 298 K

Table 1 Parameters for the Langmuir and Freundlich isotherm models

Biosorbent	Langmuir model			Freundlich model		
	Q_{max} (mg/g)	b (L/mg)	R^2	K_F ($mg^{1-n}L^n/g$)	n	R^2
A. oryzae	389.07	0.037	0.998	35.078	0.479	0.960
Mutated *A. oryzae*	627.37	0.035	0.998	38.240	0.608	0.986

equilibria, data points were fitted with Langmuir and Freundlich models [37]:

$$Q = b \times Q_{max} \times C_e/(1 + b \times C_e) \quad (1)$$

$$Q = K_F \times C_e^n \quad (2)$$

Q_{max} is theoretical maximum accumulation capacity per unit weight of the biosorbent. K_F and b are accumulation constants of Freundlich and Langmuir, respectively. In addition, n represents the Freundlich linearity index. As shown in Fig. 4b, the Langmuir model fit the experimental data better than Freundlich model. From Table 1, the Q_{max} values of U(VI) on mutated *A. oryzae* was 627.4 mg/g at 298 K, which was higher than U(VI) onto other biomaterials, such as *Algae*, *Trichoderma harzianum*, and *Catenella repens* (Table 2) [38–49]. These results indicate that mutated *A. oryzae* can be potentially used as a high efficient biomaterial in the radioactive wastewater treatment.

FTIR analysis

The FTIR spectrum of mutated *A. oryzae* was studied to evaluate the functional groups on fungal mycelia for U(VI) accumulation. In Fig. 5a exhibits the intense peaks at 3450–3200 cm^{-1} (O–H and N–H stretching vibrations), 2928–2857 cm^{-1} (C–H stretching vibrations), 1735 cm^{-1} (>C=O stretching of the protonated carboxylic or ester groups or fatty acids), 1710 cm^{-1} (C=O of COOH attributed to the amino acid), 1653 cm^{-1} (the amide I band, C=O stretching in the protein), 1557 cm^{-1} (the amide II band, C–N stretching and N–H bending vibrations associated with the protein), 1239 cm^{-1} (the amide III band, C–N stretch attributed to the protein), and 1318 cm^{-1} (C–O stretches in the lipid) [1, 50]. After U(VI) accumulation, some adsorption peaks shifted, especially, O–H and N–H stretching and carboxyl groups (C–O). Two peaks ranged from 30.6 and 41 cm^{-1} after U(VI) accumulation, which indicated that these groups were involved in accumulation process [31]. The FTIR results reveal that hydroxyl, amino, and carboxyl groups probably contribute to the complexation between U(VI) and mycelia.

XPS analysis

The XPS technique is applied to investigate U(VI) accumulation mechanism on mutated *A. oryzae*. The total scans of XPS spectra for fungus before and after accumulation

Table 2 Comparison of maximum accumulation capacities of U(VI) on various biomaterials

Biosorbents	Experimental conditions	Q_{max} (mg/g)	Reference
Algae RD256		363.1	
Algae RD257	pH = 4.5, T = 301 K	426.6	[38]
Trichoderma harzianum		496.0	
Sunflower straw	pH = 5.0, T = 298 K	251.5	[39]
Catenella repens	pH = 4.5, T = 303 K	303	[40]
Coir pith	pH = 3–6	232.56	[41]
Penicillium citrinum	pH = 6, T = 298 K	255.1	[42]
Rhodotorula glutinis	pH = 6, T = 298 K	187	[43]
Formaldehyde-treated *Rhodotorula glutinis*	pH = 6, T = 298 K	360	[43]
The amidoxime modifed *Aspergillus niger*	pH = 5, T = 298 K	621	[44]
Marine algae and yeast immobilized silica gel	pH = 4.0, T = 303 K	56.7	[45]
Eichhornia crassipes	pH = 5.5	142.85	[46]
Amidoxime-modified	pH = 5.0, T = 298 K	370.4	[47]
Spirulina platensis			
Spirulina platensis		114.9	
Chlamydomonas reinhardtii	pH = 4.5, T = 298 K	344.9	[48]
Amidoxime modified Trametes trogii	pH = 5.0, T = 298 K	447.4	[49]
A. oryzae	pH = 5.5, T = 298 K	389.07	This study
Mutated *A. oryzae*	pH = 5.5, T = 298 K	627.37	This study

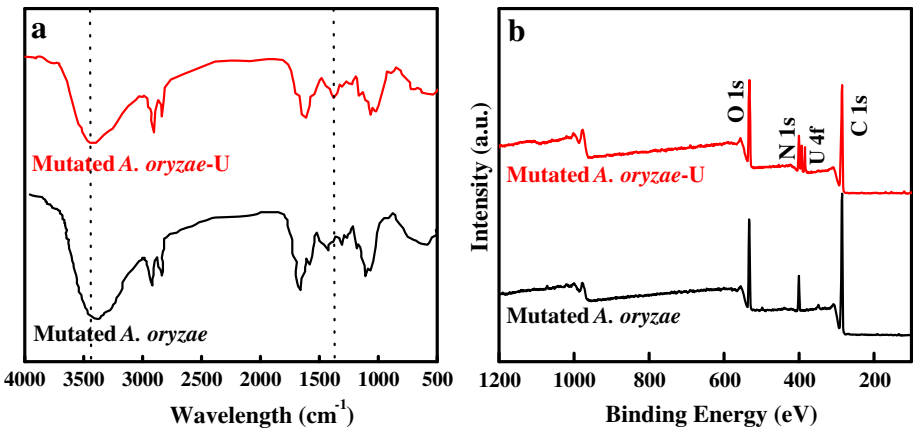

Fig. 5 FTIR spectra of mutated *A. oryzae* and mutated *A. oryzae*-U (**a**); XPS survey scan and high resolution spectra of mutated *A. oryzae* and mutated *A. oryzae*-U, total survey scans spectra (**b**), pH = 5.5, m/V = 0.6 g/l, $C_{[U(VI)]initial}$ = 50 mg/l

U(VI) are shown in Fig. 5b. After accumulation, the characteristic peak of U $4f_{7/2}$ appears at 382.3 eV, which demonstrates the high absorbability of mutated *A. oryzae*. Compared to free mutated *A. oryzae*, atomic contents (%) of C, O, and N of mutated *A. oryzae*-U correspondingly decline (Table 3). The high-resolution XPS O 1s and N 1s spectra of mutated *A. oryzae* and mutated *A. oryzae*-U are shown in Fig. 6a, b, and the results of relevant fitted peaks are listed in Table 3. The O 1s spectrum is decomposed into bridging-OH at 531.1 eV, C=O at 532.2 eV, and alcoholic C–O at 533.1 eV (Fig. 6a) [35]. Compared to mutated *A. oryzae*, the bridging-OH observably appears, and quantification of C=O and C–O bands of mutated *A. oryzae*-U reduce accordingly. Thereby, U(VI) accumulation on mutated *A. oryzae* may be due to the interaction of

Table 3 Atomic contents (%) and curve fitting results of mutated *A. oryzae* and mutated *A. oryzae*-U calculated from the XPS data

Element	Assignments	*A. oryzae*		*A. oryzae*-U	
		BE (eV)	%	BE (eV)	%
O 1s	Bridging-OH	531.1	0.07	531.2	3.76
	C=O	532.2	10.94	532.3	8.22
	C–O	533.1	9.65	533.2	7.54
Total O			20.66		19.52
N 1s	–NH–	399.9	4.83	400.0	3.32
	$–NH_2^+–$	401.9	0.12	402.1	1.27
Total N			4.95		4.57
Total C			73.94		71.88
Total P			0.45		0.47
U					3.56

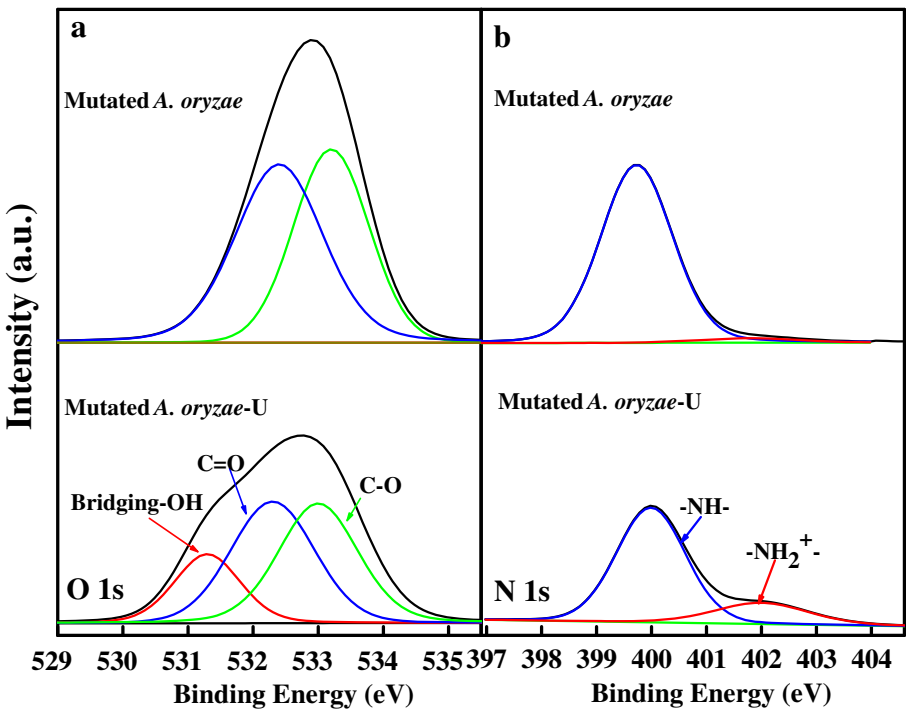

Fig. 6 XPS high resolution spectra of mutated *A. oryzae*-U, O 1s spectra (**a**), N 1s spectra (**b**)

U(VI) with OH groups on fungal mycelia [51]. Before U(VI) accumulation, only one N 1s fitted band appears at 399.9 eV, which is due to the N atom from amines and amides. After U(VI) accumulation, however, a new weak N 1s band appears at around 402.1 eV, indicating that protonated amines (–NH_2^+–) occur [52], which is attributed to the formation of R–NH_2–U(VI) complexes (Fig. 6b) [53]. Based on XPS spectra analysis, the high adsorbability of mutated *A. oryzae* is greatly due to a large number of nitrogen- and oxygen-containing functional groups on the surface of mycelia, which can easily form complexes with radionuclides.

Conclusions

To conclude, radionuclides-resistant *A. oryzae* was isolated from radionuclides contaminated soils, and the mutagenesis of *A. oryzae* by DBD plasma was greatly improved bioremediation capability of U(VI) pollution. FTIR and XPS analysis indicated that abound nitrogen- and oxygen-containing functional groups existed on mutated *A. oryzae* surfaces which accounted for U(VI) accumulation on mutated *A. oryzae*. Accumulation data can be represented by Langmuir isotherm from isotherm analysis, and mutated *A. oryzae* presented higher adsorbability for U(VI). These results show that mutated *A. oryzae* demonstrates its promising prospects of application in the treatment of radionuclides pollution in the near future.

Acknowledgments This research was supported by National Natural Science Foundation of China (21 577 032), China Postdoctoral Science Foundation funded project (2015M581047), the Priority Academic Program Development of Jiangsu Higher Education Institutions, the Collaborative Innovation Center of Radiation Medicine of Jiangsu Higher Education Institutions are acknowledged.

References

1. Mezaguer M, el hayet Kamel N, Lounici H, Kamel Z (2013) Characterization and properties of *Pleurotus mutilus* fungal biomass as adsorbent of the removal of uranium (VI) from uranium leachate. J Radioanal Nucl Chem 295:393–403
2. Miller AW, Wang Y (2012) Radionuclide interaction with clays in dilute and heavily compacted systems: a critical review. Environ Sci Technol 46:1981–1994
3. Sheng GD, Yang Q, Peng F, Li H, Gao X, Huang Y (2014) Determination of colloidal pyrolusite, Eu(III) and humic substance interaction: a combined batch and EXAFS approach. Chem Eng J 245:10–16
4. Yu SJ, Wang XX, Tan XL, Wang XK (2015) Sorption of radionuclides from aqueous systems onto graphene oxide-based materials: a review. Inorg Chem Front 2:593–612
5. Kim KW, Baek YJ, Lee KY, Chung DY, Moon JK (2015) Treatment of radioactive waste seawater by coagulation–flocculation method using ferric hydroxide and poly acrylamide. J Nucl Sci Technol 53:439–450
6. Prakash D, Gabani P, Chandel AK, Ronen Z, Singh OV (2013) Bioremediation: a genuine technology to remediate radionuclides from the environment. Microb Biotechnol 6:349–360
7. Burnett JL, Croudace IW, Warwick PE (2012) Pre-concentration of short-lived radionuclides using manganese dioxide precipitation from surface waters. J Radioanal Nucl Chem 292:25–28
8. Sheng GD, Dong HP, Shen RP, Li YM (2013) Microscopic insights into the temperature-dependent adsorption of Eu(III) onto titanate nanotubes studied by FTIR, XPS, XAFS and batch technique. Chem Eng J 217:486–494
9. Mulyutin VV, Gelis VM, Nekrasova NA, Kononenko OA, Vezentsev AI, Volovicheva NA, Korol'kova SV (2012) Sorption of Cs, Sr, U, and Pu radionuclides on natural and modified clays. Radiochemistry 54:75–78
10. Ding CC, Feng S, Cheng W, Zhang J, Li X, Liao J, Liu N (2014) Biosorption behavior and mechanism of thorium on *Streptomyces sporoverrucosus* dwc-3. J Radioanal Nucl Chem 301:237–245
11. Hassan KF, Spellerberg S, Scholten B, Saleh ZA, Qaim SM (2014) Development of an ion-exchange method for separation of radioiodine from tellurium and antimony and its application to the production of ^{124}I via the ^{121}Sb (α, n)-process. J Radioanal Nucl Chem 302:689–694
12. Ambashta RD, Sillanpää ME (2012) Membrane purification in radioactive waste management: a short review. J Environ Radioact 105:76–84
13. Reddad Z, Gerente C, Andres Y, Cloirec PL (2002) Adsorption of several metal ions onto a low-cost biosorbent: kinetic and equilibrium studies. Environ Sci Technol 36:2067–2073
14. Thatoi H, Das S, Mishra J, Rath BP, Das N (2014) Bacterial chromate reductase, a potential enzyme for bioremediation of hexavalent chromium: a review. J Environ Manage 146:383–399
15. Sathyavathi S, Manjula A, Rajendhran J, Gunasekaran P (2014) Extracellular synthesis and characterization of nickel oxide nanoparticles from *Microbacterium* sp. MRS-1 towards bioremediation of nickel electroplating industrial effluent. Bioresource Technol 165:270–273
16. Chubar N, Visser T, Avramut C, de Waard H (2013) Sorption and precipitation of Mn^{2+} by viable and autoclaved *Shewanella putrefaciens*: effect of contact time. Geochim Cosmochim Acta 100:232–250
17. Moon EM, Peacock CL (2013) Modelling Cu (II) adsorption to ferrihydrite and ferrihydrite–bacteria composites: deviation from additive adsorption in the composite sorption system. Geochim Cosmochim Acta 104:148–164
18. Zhang Y, Liu W, Xu M, Zheng F, Zhao M (2010) Study of the mechanisms of Cu^{2+} biosorption by ethanol/caustic-pretreated baker's yeast biomass. J Hazard Mater 178:1085–1093
19. Kocaoba S, Arısoy M (2011) The use of a white rot fungi (*Pleurotus ostreatus*) immobilized on Amberlite XAD-4 as a new biosorbent in trace metal determination. Bioresour Technol 102:8035–8039
20. Sánchez JG, Marrugo JL, Urango ID (2014) Simultaneous biosorption of lead and cadmium from aqueos solution by fungal biomass *Penicillium* sp. Rev Temas Agrar 19:65–74
21. Kłos A, Rajfur M (2013) Influence of hydrogen cations on kinetics and equilibria of heavy-metal sorption by algae—sorption of copper cations by the alga *Palmaria palmata* (Linnaeus) Weber & Mohr (Rhodophyta). J Appl Phycol 25:1387–1394
22. Ma Y, Wang Z, Zhu M, Yu C, Cao Y, Zhang D, Zhou G (2013) Increased lipid productivity and TAG content in Nannochloropsis by heavy-ion irradiation mutagenesis. Bioresour Technol 136:360–367
23. Sun J, Li Q, Wang Y, Zhou Z, Ding D (2015) Isolation of a strain of penicillium funiculosum, and mutational improvement for UO_2^{2+}, adsorption. J Radioanal Nucl Chem 303:427–432

24. Laroussi M, Richardson JP, Dobbs FC (2002) Effects of nonequilibrium atmospheric pressure plasmas on the heterotrophic pathways of bacteria and on their cell morphology. Appl Phys Lett 81:772–774
25. Zhang X, Zhang XF, Li HP, Wang LY, Zhang C, Xing XH, Bao CY (2014) Atmospheric and room temperature plasma (ARTP) as a new powerful mutagenesis tool. Appl Microbiol Biotechnol 98:5387–5396
26. Huixia C, Zhilong X, Fengwu B (2014) Improved Ethanol Production from Xylose by Candida shehatae Induced by Dielectric Barrier Discharge Air Plasma. Plasma Sci Technol 16:602–607
27. Dong XY, Xiu ZL, Li S, Hou YM, Zhang DJ, Ren CS (2010) Dielectric barrier discharge plasma as a novel approach for improving 1, 3-propanediol production in *Klebsiella pneumoniae*. Biotechnol Let 32:1245–1250
28. Wang LY, Huang ZL, Li G, Zhao HX, Xing XH, Sun WT (2010) Novel mutation breeding method for streptomyces avermitilis, using an atmospheric pressure glow discharge plasma. J Appl Microbiol 108:851–858
29. Qi F, Kitahara Y, Wang Z, Zhao X, Du W, Liu D (2014) Novel mutant strains of Rhodosporidium toruloides by plasma mutagenesis approach and their tolerance for inhibitors in lignocellulosic hydrolyzate. J Chem Technol Biotechnol 89:735–742
30. Masneuf-Pomarède I, Le Jeune C, Durrens P, Lollier M, Aigle M, Dubourdieu D (2007) Molecular typing of wine yeast strains *Saccharomyces bayanus* var. *uvarum* using microsatellite markers. Syst Appl Microbiol 30:75–82
31. Kumar R, Bhatia D, Singh R, Bishnoi NR (2012) Metal tolerance and sequestration of Ni (II), Zn (II) and Cr(VI) ions from simulated and electroplating wastewater in batch process: kinetics and equilibrium study. Int Biodeter Biodegr 66:82–90
32. León-Santiesteban HH, Wrobel K, García LA, Revah S, Tomasini A (2014) Pentachlorophenol sorption by *Rhizopus oryzae* ENHE: pH and temperature effects. Water Air Soil Poll 225:1–10
33. Strawn DG, Sparks DL (1999) The use of XAFS to distinguish between inner- and outer-sphere lead adsorption complexes on montmorillonite. J Colloid Interf Sci 216:257–269
34. Sheng GD, Hu J, Alsaedi A, Shammakh W, Monaquel S, Ye F, Ahmad B (2015) Interaction of uranium(VI) with titanate nanotubes by macroscopic and spectroscopic investigation. J Mol Liq 212:563–568
35. Song WC, Wang XX, Wang Q, Shao DD, Wang XK (2015) Plasma-induced grafting of polyacrylamide on graphene oxide nanosheets for simultaneous removal of radionuclides. Phys Chem Chem Phys 17:398–406
36. Zhao GX, Li JX, Ren XM, Chen CL, Wang XK (2011) Few-layered graphene oxide nanosheets as superior sorbents for heavy metal ion pollution management. Environ Sci Technol 45:10454–10462
37. Chen YT, Zhang W, Yang SB, Hobiny A, Alsaedi A, Wang XK (2016) Understanding the adsorption mechanism of Ni(II) on graphene oxides by batch experiments and density functional theory studies. Sci China Chem 59:412–419
38. Akhtar K, Waheed Akhtar M, Khalid AM (2007) Removal and recovery of uranium from aqueous solutions by *Trichoderma harzianum*. Water Res 41:1366–1378
39. Ai L, Luo X, Lin X, Zhang S (2013) Biosorption behaviors of uranium (VI) from aqueous solution by sunflower straw and insights of binding mechanism. J Radioanal Nucl Chem 298:1823–1834
40. Bhat SV, Melo JS, Chaugule BB, D'souza SF (2008) Biosorption characteristics of uranium (VI) from aqueous medium onto *Catenella repens*, a red alga. J Hazard Mater 158:628–635
41. Parab H, Joshi S, Shenoy N, Verma R, Lali A, Sudersanan M (2005) Uranium removal from aqueous solution by coir pith: equilibrium and kinetic studies. Bioresour Technol 96:1241–1248
42. Pang C, Liu YH, Cao XH, Li M, Huang GL, Hua R, Wang CX, Liu YT, An XF (2011) Biosorption of uranium (VI) from aqueous solution by dead fungal biomass of *Penicillium citrinum*. Chem Eng J 170:1–6
43. Bai J, Yao HJ, Fan FL, Lin MS, Zhang LN, Ding HJ, Lei FA, Wu XL, Li XF, Guo JS, Qin Z (2010) Biosorption of uranium by chemically modified *Rhodotorula glutinis*. J Environ Radioactiv 101:969–973
44. Li L, Hu N, Ding D, Xin X, Wang Y, Xue J, Tan Y (2015) Adsorption and recovery of U(vi) from low concentration uranium solution by amidoxime modified *Aspergillus niger*. RSC Adv 5:65827–65839
45. Aytas S, Turkozu DA, Gok C (2011) Biosorption of uranium(VI) by bi-functionalized low cost biocomposite adsorbent. Desalination 280:354–362
46. Yi ZJ, Yao J, Chen HL, Wang F, Yuan ZM, Liu X (2016) Uranium biosorption from aqueous solution onto *Eichhornia crassipes*. J Environ Radioact 154:43–51
47. Bayramoglu G, Akbulut A, Arica MY (2015) Study of polyethyleneimine-and amidoxime-functionalized hybrid biomass of *Spirulina (Arthrospira) platensis* for adsorption of uranium (VI) ion. Environ Sci Pollut R 22:17998–18010
48. Erkaya IA, Arica MY, Akbulut A, Bayramoglu G (2014) Biosorption of uranium (VI) by free and entrapped *Chlamydomonas reinhardtii*: kinetic, equilibrium and thermodynamic studies. J Radioanal Nucl Chem 299:1993–2003
49. Bayramoglu G, Arica MY (2016) Amidoxime functionalized *Trametes trogii* pellets for removal of uranium (VI) from aqueous medium. J Radioanal Nucl Chem 307:373–384
50. Doshi H, Ray A, Kothari IL (2007) Biosorption of cadmium by live and dead Spirulina: IR spectroscopic, kinetics, and SEM studies. Curr Microbiol 54:213–218
51. Tan XL, Fang M, Li JX, Lu Y, Wang XK (2009) Eu(III) sorption to TiO_2 (anatase and rutile): batch, XPS, and EXAFS studies. Environ Sci Technol 168:458–465
52. Yuan SJ, Sun M, Sheng GP, Li Y, Li WW, Yao RS, Yu HQ (2010) Identification of key constituents and structure of the extracellular polymeric substances excreted by *Bacillus megaterium* TF10 for their flocculation capacity. Environ Sci Technol 45:1152–1157
53. Jin L, Bai R (2002) Mechanisms of lead adsorption on chitosan/PVA hydrogel beads. Langmuir 18:9765–9770